Journal of Chemical&Engineering Data

pubs.acs.org/jced

Article

Phase Diagram and Thermodynamic Properties of the $EuBr_2$−CsBr Binary System

Leszek Rycerz,* Jan Kapała, and Marcelle Gaune-Escard

Cite This: *J. Chem. Eng. Data* 2021, 66, 1939−1946

Read Online

ACCESS | Metrics & More | Article Recommendations

ABSTRACT: Phase equilibria in the $EuBr_2$−CsBr binary system were investigated by the differential scanning calorimetry method. The mixing enthalpy of the liquid phase at 1055 K was measured using a Calvet calorimeter over the whole composition range. Two compounds, $CsEuBr_3$, congruently melted at 1034 K, and $CsEu_3Br_7$, decomposed at 704 K, were found in the solid phase. Two eutectics were located at x_{EuBr_2} = 0.197 (T = 812 K) and x_{EuBr_2} = 0.821 (T = 864 K). The heat capacities of solid and liquid phases of $CsEuBr_3$ were measured from 300 to 1100 K. The CALPHAD method was used to verify the thermodynamic phase compatibility of the system. The Gibbs free energy of formation of solid compounds was calculated.

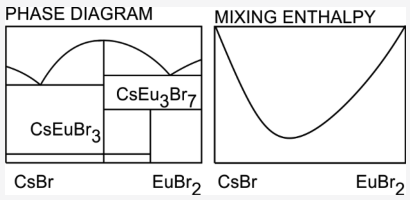

1. INTRODUCTION

"The photoluminescence properties of divalent lanthanides have attracted a lot of attention both from theoretical and applicational perspectives due to the parity-allowed character of the 5d−4f transitions they exhibit in the UV and visible range. Among them, Eu^{2+} is by far the most studied ion due to its rather high stability and the fact that it shows luminescence in essentially any visible color solely dependent on the appropriate choice of the respective host compound".[1] "Compositions based on CsBr:Eu^{2+} are considered as the perspective storage X-ray phosphors for visualization of the X-ray images or luminophore plate production".[2,3] These phosphors can be produced by a vacuum evaporation method,[4] in which the mixture of CsBr and $EuBr_2$ is used as the phosphor raw material.[5] "In the formation of a vacuum-evaporated layer using vapor phase sedimentation, the melting point of a phosphor raw material decreases due to an activator ($EuBr_2$) added to the phosphor host crystal CsBr".[4] Thus, the knowledge of the phase equilibria in the CsBr−$EuBr_2$ system seems to be useful in the production of discussed above phosphors. Therefore, we decided to investigate these phase equilibria and they are presented in this work.

2. EXPERIMENTAL SECTION

2.1. Chemical Reagents. The main reagents used in this study are listed in Table 1.

Europium(II) bromide was synthesized from the oxide Eu_2O_3 (Aldrich 99.9%) by a modified Haschke and Eick method.[6] The main steps of the synthesis included dissolution of europium oxide in hot concentrated hydrobromic acid, crystallization of europium bromide hexahydrate, dehydration of bromide hexahydrate by slow heating up to 570 K in the presence of ammonium bromide, sublimation of unreacted ammonium bromide, and decomposition of europium(III) bromide under vacuum (about 1 Pa) at a temperature of 770 K. Chemical analysis of obtained $EuBr_2$ performed by mercurimetric (bromine) and complexometric (europium) methods confirmed its good quality (Eu, 48.74% found, 48.75% calcd; Br, 51.26% found, 51.25% calcd).

Table 1. Reagents Used in the Studies

reagent	source	purity (w/w %)	CAS no.
Eu_2O_3	Sigma-Aldrich	99.9	1308-96-9
$EuBr_2$	synthesis[a]	99.9	13780-48-8
HBr	Sigma-Aldrich	48	10035-10-6
NH_4Br	Sigma-Aldrich	99.0	12124-97-9
CsBr	Sigma-Aldrich	Suprapur (min. 99.9)	7787-69-1
$CsEuBr_3$	synthesis	99.9	

[a]Content of bromine and europium determined by mercurimetric and complexometric methods, respectively.

Cesium bromide (Merck Suprapur reagent, min. 99.9%) was dried in a gaseous HBr atmosphere.

Mixtures of $EuBr_2$ and CsBr (in appropriate proportions) were melted in vacuum-sealed quartz ampoules, homogenized, and solidified. The $CsEuBr_3$ stoichiometric compound was prepared in the same way. The mass of samples used in differential scanning calorimetry (DSC) experiments varying in the range of 300−400 mg. However, 3−4 g of each mixture was prepared in order to avoid deviation from stoichiometry.

Received: December 4, 2020
Accepted: April 2, 2021
Published: April 19, 2021

The samples were prepared and stored in a glove box under an atmosphere of pure argon (water content: <1 ppm).

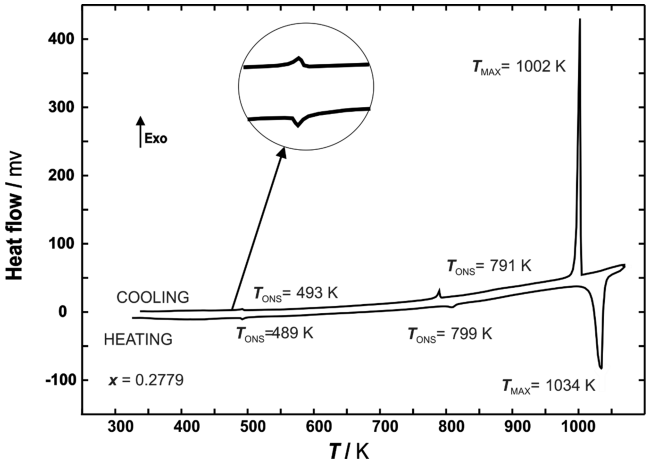

Figure 1. DSC heating and cooling curves for the $EuBr_2$−CsBr mixture with a mole fraction of $EuBr_2$ x = 0.278.

2.2. Measuring Instruments. The DSC experiments were performed with a Setaram DSC 121 differential scanning calorimeter equipped with 3D DSC sensor. The advantages of this sensor compared to the 2D sensor, as well as the procedure for calibrating the apparatus and measurements, were presented in earlier publications.[7−9]

The heat capacity of $CsEuBr_3$ compound was measured with the same Setaram DSC 121 by a so-called step method described in detail previously.[8,9]

In heat capacity experiments, each 5 K heating step was followed by a 400 s isothermal delay. The heating rate was 1.5 $K \cdot min^{-1}$. The mass difference of the quartz cells in any individual experiment did not exceed 1 mg (cell mass: 400−500 mg).

The mixing experiments were all of the simple liquid−liquid type, performed under pure argon at atmospheric pressure. The Calvet-type high-temperature microcalorimeter, the mixing device, and the "break-off bubble" experimental method have all been described in detail elsewhere.[8,9] Calibration of the calorimeter was performed with α-alumina obtained from NIST. After the mixing experiments, pieces of α-alumina (30−100 mg) were dropped into the melt and the corresponding enthalpy increment was measured.

2.3. Experimental Uncertainty. The standard experimental deviations as well as the standard uncertainties were determined using the Guide to the Expression of Uncertainty in Measurements (GUM).[10] The standard uncertainty in mole fraction composition was thus estimated using

$$u^2(x_{EuBr_2}) = [x_{EuBr_2} \cdot (1 - x_{EuBr_2})] \cdot [u_r^2(n_{EuBr_2}) + u_r^2(n_{CsBr})] \quad (1)$$

The standard uncertainty in n_{EuBr_2} and n_{CsBr} was estimated by combining the squared uncertainty of the $EuBr_2$ and CsBr mass measurement and the purity of these compounds as specified in Table 1.

The standard uncertainty of the temperature measurements was estimated by combining in quadrature the standard deviation of five repeat measurements performed with high-purity metals (0.8 K) with the standard uncertainty of the thermocouple calibration (0.6 K).

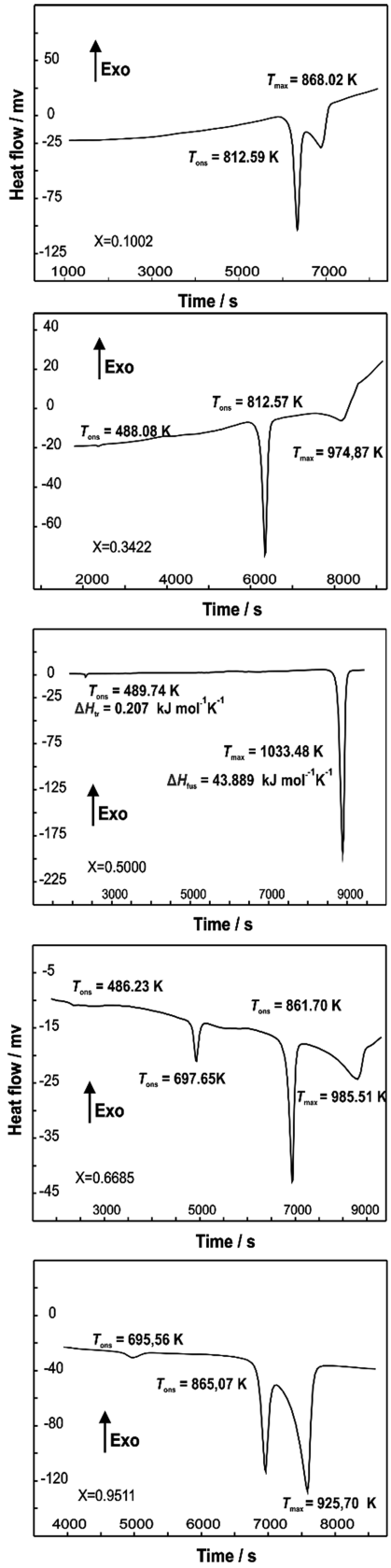

Figure 2. Selected DSC heating curves of $EuBr_2$−CsBr mixtures.

The relative uncertainty of mixing enthalpy determination ($u_r(\Delta_{mix}H_m)$ = 0.08) was discussed in detail in our previous

https://doi.org/10.1021/acs.jced.0c01016
J. Chem. Eng. Data 2021, 66, 1939−1946

work.[11] Determined in a similar manner, relative uncertainties of enthalpy of phase transition, ($u_r(\Delta_{trs}H_m)$), and fusion, ($u_r(\Delta_{fus}H_m)$), were 0.04 and 0.016, respectively.

3. RESULTS AND DISCUSSION

3.1. $EuBr_2$−CsBr Phase Diagram. DSC cooling curves of all samples under investigation showed the supercooling effect

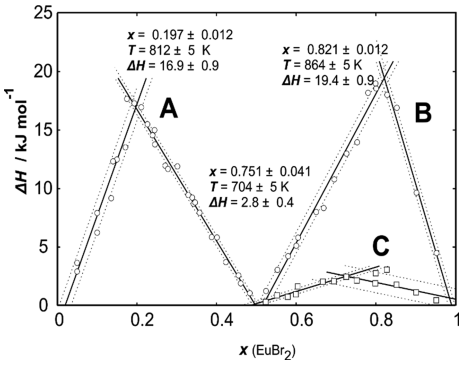

Figure 3. Tammann diagrams for determination: (A) CsBr−$CsEuBr_3$ eutectic, (B) $CsEuBr_3$−$EuBr_2$ eutectic, and (C) stoichiometry of the $CsEu_3Br_7$ compound.

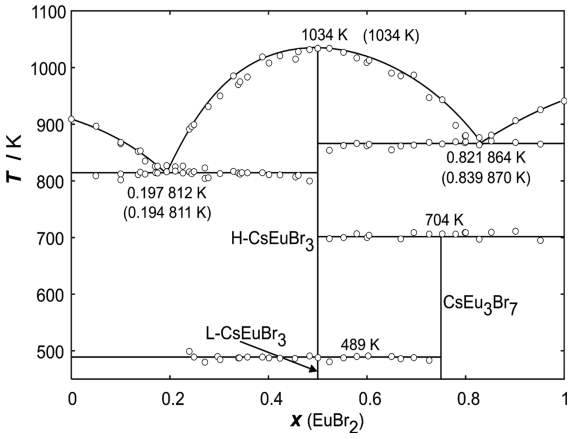

Figure 4. Phase diagram of the $EuBr_2$−CsBr binary system: circles and values without parenthesis, experimental data; lines and values in parenthesis, data calculated by the CALPHAD method.

(from several to several tens of Kelvin), as exemplified in Figure 1. Therefore, all the temperature and enthalpy values were determined from heating curves. Temperatures of the effects (formation, transition, and fusion) were determined as onset extrapolated temperatures (T_{onset}), whereas these related to the liquidus were determined as peak maximum temperatures.

In all thermograms, the endothermic effect observed at the highest temperature corresponds to liquidus. Two or three endothermic effects were observed over the entire composition range in addition to liquidus effect (Figure 2).

The first, at 812 K (mean value from measurements), was visible in all thermograms up to $x < 0.500$, where x is the $EuBr_2$ mole fraction. Its disappearance at $x = 0.500$ suggests the existence of the $CsEuBr_3$ compound. Accordingly, the effect under discussion can be attributed to the CsBr−$CsEuBr_3$ eutectic. Its composition was determined from the so-called Tammann diagram.[12,13] The importance of this diagram was discussed in detail by Dańczak and Rycerz.[14] The Tammann

Table 2. DSC Results for the $EuBr_2$−CsBr Binary System[a]

$x(EuBr_2)$	$CsEuBr_3$ trans. T/K	$CsEu_3Br_7$ decomposition T/K	CsBr−$CsEuBr_3$ eutectic T/K	$CsEuBr_3$−$EuBr_2$ eutectic T/K	liquidus T/K
0.0000					909
0.0497			809		
0.0499			809		897
0.1002			812		868
0.1007			802		866
0.1355			811		852
0.1401			815		853
0.1497			812		835
0.1710			816		825
0.1749			814		826
0.1934			816		827
0.2109			817		825
0.2264			814		826
0.239	499		816		891
0.2394			813		896
0.2489	490		816		899
0.2709	480		804		923
0.2778			805		931
0.2972	490				
0.3018	485		813		950
0.329			817		985
0.3289	488		814		970
0.3422	488		812		975
0.3460			814		
0.357	489		814		983
0.3877	490		814		1019
0.4010	488		811		1008
0.4233	487		811		1021
0.4549	487		807		1015
0.4605			809		1028
0.4835	491		800		1032
0.5001	489				1034
0.5007	488				
0.5241	481	698		854	1034
0.5523	488	700		863	1027
0.5792	490	707		866	1017
0.5996	489	701		862	1009
0.6041	490	704		865	1013
0.6496	490			855	990
0.6685	486	698		862	985
0.6950	488	709		863	987
0.7261	486	706		868	947
0.7526		706		865	943
0.7798		706		869	898
0.7988		709		868	879
0.8000		709		869	879
0.8278		697		864	876
0.8522		710		870	881
0.9014		711		868	906
0.9518		696		865	926
1.0000					941

[a] p = 2 Pa, standard uncertainties u are $u(T)$ = 5 K, $u(x)$ = 0.0005, and $u_r(p)$ = 0.50.

diagram, i.e., dependence of enthalpy related to the effect at 812 K (calculated per mole of mixture) on the mole fraction of $EuBr_2$, is presented in Figure 3 (graph A). It gives the composition of the CsBr−$CsEuBr_3$ eutectic as $x = 0.197 \pm$

https://doi.org/10.1021/acs.jced.0c01016
J. Chem. Eng. Data 2021, 66, 1939−1946

Table 3. Heat Capacity of the $CsEuBr_3$ Compound[a]

T/K	Cp/J/(mol·K)	T/K	Cp/J/(mol·K)	T/K	Cp/J/(mol·K)	T/K	Cp/J/(mol·K)
L-$CsEuBr_3$ (solid)		520	148.7	644	150.5	868	156.6
306	155.5	525	148.8	649	150.9	873	157.3
311	154.4	530	148.6	654	152.3	877	157.6
316	157.5	535	146.4	659	152.2	882	158.1
321	155.5	540	146.9	664	151.0	887	157.2
326	153.9	545	147.6	669	151.3	892	154.9
331	152.3	549	148.1	674	149.3	897	156.9
336	152.8	554	148.0	679	150.9	902	159.6
341	152.3	559	148.8	684	149.0	907	155.4
346	152.8	564	148.1	689	148.9	912	155.5
351	154.6	569	148.9	694	149.5	917	156.0
356	154.3	574	148.4	699	149.9	922	156.8
361	155.6	579	149.2	704	149.6	927	156.9
366	155.8	584	148.5	709	151.7	932	161.0
371	156.6	589	149.1	714	151.3	937	156.7
376	156.4	594	149.4	719	152.7	942	161.0
381	156.6	599	150.0	724	152.5	947	158.8
386	157.3	604	149.7	729	151.1	952	156.4
391	159.7	609	150.0	734	150.3	957	158.6
396	157.3	614	149.7	739	151.6	962	162.2
401	157.4	619	148.7	743	151.2	967	160.0
406	157.4	624	147.6	748	151.4	972	161.4
411	158.3	629	148.7	753	151.6	977	163.4
415	157.6	634	155.2	758	150.7	982	169.0
420	158.3	639	153.8	763	152.1	987	165.0
425	161.2	644	153.0	768	152.0	992	167.7
430	162.6	649	153.4	773	153.3	997	172.4
435	163.6	654	153.9	778	153.6	1002	175.6
440	154.4	659	152.7	783	154.1	1007	182.9
445	154.2	664	152.8	788	154.4	1011	203.1
450	152.9	669	151.9	793	155.0	1016	272.4
455	153.7	674	152.0	798	156.2	1021	595.1
460	152.9	678	151.2	803	154.1	1026	3687.3
465	153.7	683	152.0	808	154.6	1031	2362.8
470	155.3	688	151.2	813	155.1	$CsEuBr_3$ (liquid)	
475	157.3	693	149.7	818	157.5	1041	205.3
480	158.1	698	148.9	823	156.5	1046	202.7
485	160.6	703	148.0	828	154.6	1051	207.1
H-$CsEuBr_3$ (solid)		708	147.7	833	155.9	1056	210.9
490	204.7	713	148.4	838	155.4	1061	209.6
495	155.5	718	147.5	843	158.1	1066	214.0
500	141.0	723	147.2	848	155.7	1071	206.8
505	148.9	728	146.4	853	156.3	1076	209.8
510	148.5	733	147.5	858	155.1	1081	209.8
515	147.9	738	147.0	863	159.9	1086	207.6

[a] p = 2 Pa, standard uncertainties u are: $u(T)$ = 1 K, $u(x)$ = 0.0005, $u_r(Cp)$ = 0.02, and $u_r(p)$ = 0.50.

0.012. The eutectic mixture melts with enthalpy , $\Delta_{fus}H_m$, of about 16.9 ± 0.9 kJ mol^{-1} at a temperature of 812 K.

In the sample with composition x = 0.500, effects at 489 and 1034 K were observed on thermograms. The effect at 1034 K had a characteristic shape, typical of a congruently melting compound. It confirms existence of congruently melting $CsEuBr_3$. The effect at 489 K can be attributed to the solid−solid phase transition of this compound.

Two thermal events were observed in the samples from the composition range 0.500 < x < 1 in addition to liquidus effect. The effect at 864 K is related to the $CsEuBr_3$−$EuBr_2$ eutectic. From the Tammann diagram (Figure 3, graph B), its composition was determined as x = 0.821 ± 0.012. This mixture melts with enthalpy, $\Delta_{fus}H_m$, of about19.4 ± 0.9 kJ mol^{-1}.

The effect at 704 K was attributed to the decomposition in the solid phase of another compound. The mole fraction of $EuBr_2$ determined from the Tammann plot (Figure 3, graph C) as x = 0.751 ± 0.041 corresponds very well to the stoichiometry of the $CsEu_3Br_7$ compound.

The effect at 489 K, appearing in the composition range 0.25 < x < 0.750, can be undoubtedly ascribed to the phase transition of $CsEuBr_3$. Due to a very small value of enthalpy of this transition (0.25 kJ mol^{-1}), this effect was not visible for the samples with a low mole fraction of $EuBr_2$ and, accordingly, it was impossible to create a Tammann diagram.

https://doi.org/10.1021/acs.jced.0c01016
J. Chem. Eng. Data 2021, 66, 1939−1946

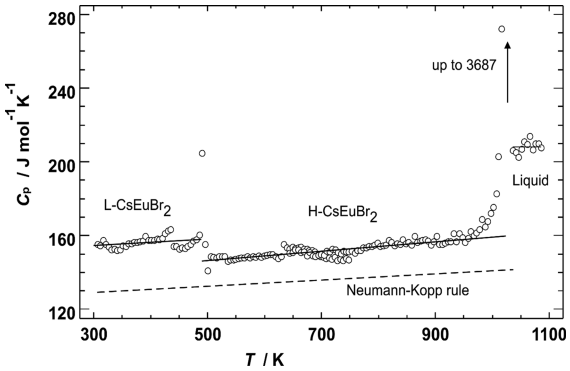

Figure 5. Molar heat capacity of $CsEuBr_3$: open circles, experimental results; solid lines, polynomial fitting of experimental results; dashed lines, heat capacity calculated by the Neumann–Kopp rule.[14]

The complete phase diagram, determined for the first time during this work, is presented in Figure 4. All of the temperatures of thermal effects of analyzed samples are presented in Table 2.

3.2. Thermodynamic Properties of the $CsEuBr_3$ Compound. As mentioned above, congruently melting the $CsEuBr_3$ compound exists in the system under investigation. It undergoes a solid–solid transition at 489 K with enthalpy $\Delta_{trs}H_m = 0.25 \pm 0.01$ kJ mol^{-1} ($u_r(\Delta_{trs}H_m) = 0.04$) and melts congruently at 1034 K with enthalpy $\Delta_{fus}H_m = 43.2 \pm 0.7$ kJ mol^{-1} ($u_r(\Delta_{fus}H_m) = 0.016$).

Experimental heat capacity data on the $CsEuBr_3$ compound (determined for the first time) are presented in Table 3 and plotted against temperature in Figure 5. Molar heat capacities of low- and high-temperature modifications of $CsEuBr_3$ were found to increase linearly with temperature. They are significantly larger than the values calculated from the Neumann–Kopp rule.[15] A constant heat capacity value C_p of 208.2 ± 3.1 J mol^{-1} K^{-1} was found for liquid $CsEuBr_3$.

A linear function of temperature

$$C_p = a + b \cdot T \tag{2}$$

was used to fit experimental data. The coefficients a and b in the above equation are listed in Table 4.

3.3. Mixing Enthalpy in the $EuBr_2$–CsBr Liquid Mixtures. The mixing enthalpies of the $EuBr_2$–CsBr liquid binary system were determined for the first time in this work. The calorimetric experiments were performed at 1055 K on samples with different compositions in the whole x_{EuBr_2} range (from 0.040 to 0.850). The results are presented in Table 5 and are plotted against composition in Figure 6.

All the melts are characterized by negative enthalpies of mixing with a minimum value of approximately −6.0 kJ·mol^{-1} at a mole fraction of $EuBr_2$ of about 0.4.

Figure 7 shows the dependence of interaction parameter λ ($\lambda = H_{MIX} \cdot x_{CsBr}^{-1} \cdot x_{EuBr_2}^{-1}$) on europium bromide mole fraction

Table 5. Molar Enthalpy of Mixing, $\Delta_{mix}H_m$, of the $EuBr_2$–CsBr Liquid System at T = 1055 K[a]

x_{EuBr_2}	$\Delta_{mix}H_m$ (kJ·mol^{-1})	x_{EuBr_2}	$\Delta_{mix}H_m$ (kJ·mol^{-1})
0.0399	−1.03	0.4072	−5.88
0.0508	−1.22	0.4697	−5.48
0.0995	−2.26	0.5078	−6.31
0.1544	−3.40	0.5418	−5.91
0.1936	−4.23	0.6148	−4.95
0.2012	−4.13	0.6555	−4.75
0.2449	−5.11	0.7049	−3.95
0.3010	−5.86	0.7447	−3.21
0.3136	−5.77	0.8110	−2.64
0.3427	−5.86	0.8499	−2.06

[a] p = 1013 hPa, standard uncertainties u are $u(x) = 0.0005$, $u(T) = 1$ K, $u_r(\Delta_{mix}H_m) = 0.08$, and $u_r(p) = 0.002$.

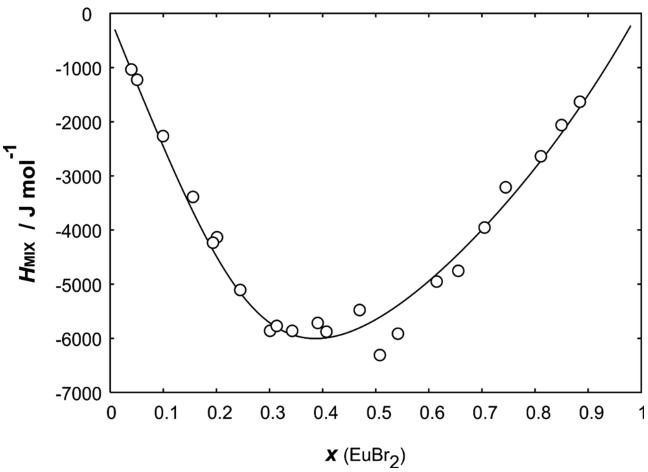

Figure 6. Molar enthalpies of mixing $\Delta_{mix}H_m$ in the $EuBr_2$–CsBr liquid systems at T = 1055 K: open circles, experimental results; solid line, obtained by the CALPHAD method.

for the system under investigation. In contrast to LnX_3–MX binary systems (Ln = lanthanide, M = alkali metal, and X = halide),[8,9] this parameter does not show a very deep minimum that suggests complex formation in these melts, similarly as in the case of $EuCl_2$–MCl liquid systems.[16] However, some neutron diffraction experiments performed on the $EuCl_2$–NaCl system[17] hint at the existence of complexes also in this system. The existence of the tetrahedral $MeCl_4^{2-}$ complex species in the melts containing alkali chloride–divalent metal chloride (such as Mn, Fe, Co, Ni, Cd, and Pb)[18−20] was also showed. All these facts suggest that some complex species may be formed in $EuBr_2$–MBr liquids. Thus, the formation of $EuBr_4^{2-}$ may also occur in $EuBr_2$–CsBr melts.

3.4. CALPHAD Calculation. "The CALPHAD approach is a semi-empirical method based on the sequential modeling of the thermodynamic properties of multicomponent systems,

Table 4. Coefficients of eq 2 Describing the Heat Capacity of $CsEuBr_3$[a]

phase	a	$\pm\Delta a$	b	$\pm\Delta b$	std. dev.	temperature range T/K
L-$CsEuBr_3$ (solid)	149.3	3.4	0.01773	0.00843	2.71	298–489
H-$CsEuBr_3$ (solid)	132.7	1.2	0.02700	0.00160	2.20	489–1034
$CsEuBr_3$ (liquid)	208.2				3.07	1034–1100

[a] std. dev. $= \sqrt{\sum \frac{(C_p(\text{experimental}) - C_p(\text{calculated}))^2}{(n-2)}}$, where n is the number of experimental points.

https://doi.org/10.1021/acs.jced.0c01016
J. Chem. Eng. Data 2021, 66, 1939−1946

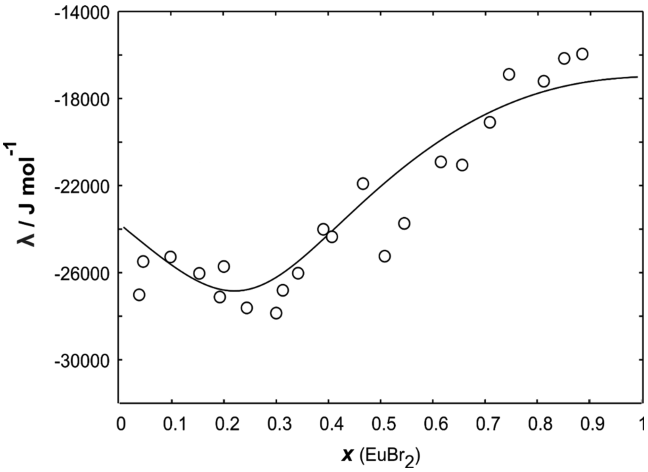

Figure 7. Dependence of interaction parameter λ on the mole fraction of europium(II) bromide at temperature T = 1055 K: open circles, experimental results; solid line, obtained by the CALPHAD method.

which needs a basic amount of experimental data for creation of consistent and reliable set of thermodynamic parameters describing simple systems".[21]

The calculations were made by BINGSS and BINFKT programs of Lukas[22,23] and the special management program PHDMAN for fast calculation by Bayes regression.[24] Experimental data obtained in this work and literature data concerning pure $EuBr_2$[25] and CsBr[26] were used in our calculations.

The temperature dependence of Gibbs free energy of pure system components was presented in form of the SGTE description:

$$\{G^0(T) - H^{SER}(298.15\ K)\}_i = A_i + B_i \cdot T + C_i \cdot T \cdot \ln T + D_i \cdot T^2 \quad (3)$$

where A_i...D_i are the coefficients presented in Table 6.

The thermodynamic properties of the liquid phase in the investigated system were modelled using the associated solution model (ASM) with one associate. A detailed description of the ASM was given by Sommer[27,28] and Krull *et al.*[29] We assumed the formation of associates according to the equation

$$2CsBr + EuBr_2 = (CsBr)_2(EuBr_2) \quad (4)$$

After the association process, the solution consists of $EuBr_2$, CsBr, and $(CsBr)_2(EuBr_2)$ associates, and the system can be treated as the pseudo-ternary $EuBr_2$−CsBr−$(CsBr)_2(EuBr_2)$ system. The total number of moles is described by eq 5:

$$n = n_{EuBr_2} + n_{CsBr} + n_a \quad (5)$$

Table 7. Calculated Coefficients of eq 6

A_1	B_1	A_2	B_2	A_3	B_3	A_4	B_4
−36,000	22.0	−17,000	1.0	6950	−11.5	8000	9.0

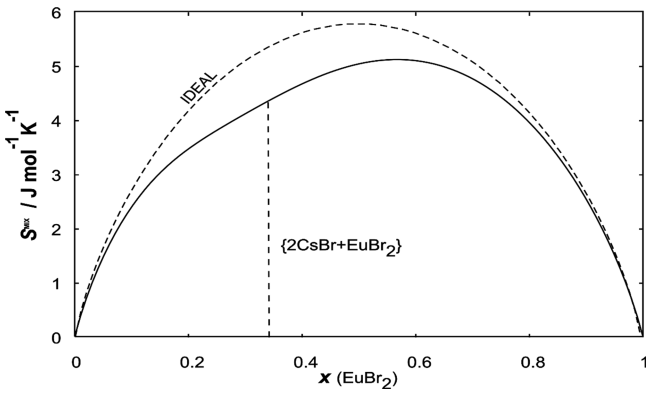

Figure 8. Dependence of calculated mixing entropy on the mole fraction of $EuBr_2$ for the liquid $EuBr_2$−CsBr mixtures: broken line, entropy of the ideal mixture.

Table 8. Coefficients of eq 8 Describing the Dependence of Gibbs Free Energy of Formation of Solid Compounds

compound	A	B	C
L-$CsEuBr_3$ (solid)	−33,760	177.8	−25.32
H-$CsEuBr_3$ (solid)	−29,518	109.0	−15.52
$CsEu_3Br_7$ (solid)	−24,880		

where n is the total number of moles, and n_{EuBr_2}, n_{CsBr}, and n_a are the number of mole of europium(II) bromide, cesium bromide, and associate, respectively.

The Gibbs free energy of mixing of liquid phase, obtained by the ASM is described by the formula

$$\begin{aligned} G^{MIX}(x, T) = {} & R \cdot T \cdot (y_{CsBr} \cdot \ln y_{CsBr} + y_{EuBr_2} \cdot \ln y_{EuBr_2}) \\ & + y_a \cdot \ln y_a)/n + (A_1 + B_1 \cdot T) \cdot y_a \cdot n \\ & + \{(A_2 + B_2 \cdot T) y_{CsBr} \cdot y_{EuBr_2} \\ & + (A_3 + B_3 \cdot T) y_{CsBr} \cdot y_a \\ & + (A_4 + B_4 \cdot T) y_{EuBr_2} \cdot y_a\}/n \end{aligned} \quad (6)$$

where A_i and B_i are the optimized coefficients, and y_{CsBr}, y_{EuBr_2}, and y_a are the mole fractions of CsBr, $EuBr_2$, and associate in the pseudo-ternary liquid $EuBr_2$−CsBr−$(CsBr)_2(EuBr_2)$ system obtained from balance equations for one mole of the liquid phase, respectively. The details of calculations were described in our previous works.[7,30] The standard deviation of the fit of liquidus line and standard deviation of the fit of mixing enthalpy were used as the

Table 6. Coefficients of eq 3 Describing the Temperature Dependence of Gibbs Free Energy of the Pure System Components (in J mol^{-1})

compound	A_i	$B_i \cdot 10^{-2}$	C_i	D_i	temperature range T/K
CsBr (solid)	−15400.3719	2.26971124	−50.38	−0.00427	298−911
CsBr (liquid)	−12871.8292	4.04434534	−77.4	0	911−1100
$EuBr_2$ (solid)	−22402.6372	3.60520024	−77.39	−0.004155	298−941
$EuBr_2$ (liquid)	−26135.5536	5.76187376	−105.39	0	941−1100

https://doi.org/10.1021/acs.jced.0c01016
J. Chem. Eng. Data 2021, 66, 1939−1946

criterion of adequacy. These values are $\Delta T^{LIQUIDUS}$ = 21 K and ΔH^{MIX} = 359 J mol^{-1}. The optimized coefficients of eq 6 are presented in Table 7.

The calculated phase diagram (line in Figure 4) is in a good agreement with the measured one (points in Figure 4).

The mixing entropy in the system investigated is significantly smaller than ideal entropy (Figure 8). It confirms the formation of associate. The value of S^{MIX} at $x(EuBr_2)$ = 0.33, corresponding to the stoichiometry of associate is equal to 4.30 J mol^{-1} K^{-1}. This value is lower than the ideal mixing entropy, where the value at this mole fraction is equal to 5.27 J mol^{-1} K^{-1}.

The estimated amount of associate obtained by the way shown in previous works[27,31] is y_a = 0.25 at $x(EuBr_2)$ = 0.33, and the equilibrium constant of the reaction of the associate formation (eq 4) expressed by the equation

$$K = y_a/(y_{CsBr}{}^2 \cdot y_{EuBr_2}) \tag{7}$$

is equal to 24.19.

The thermodynamics of solid compounds was also calculated. The heat capacity of both solid phases of the $CsEuBr_3$ compound differs significantly from the Neumann−Kopp rule (Figure 5). The mean difference between experimental and calculated by NK values was used as a fixed coefficient (C_i) in the dependence of Gibbs free energy of formation on temperature:

$$\Delta G^{FORM}(T) = A_i + B_i \cdot T + C_i \cdot T \cdot \ln(T) \tag{8}$$

All the coefficients of eq 8, obtained by the CALPHAD calculation, are shown in Table 7. The values of Gibbs free energy of formation at the whole temperature range of phase existence are significantly negative. There are not enough data to calculate the dependence of Gibbs free energy of formation on the temperature of the $CsEu_3Br_7$ compound; thus, only the value of ΔG^{FORM}(704 K) was shown in Table 8.

The negative values of Gibbs free energy of formation confirm the stability of the $CsEuBr_3$ compound. Note that stability of $CsEu_3Br_7$ is significantly lower than $CsEuBr_3$, and this agree with the fact of lower stability and decomposition in the solid phase at 704 K.

4. CONCLUSIONS

1. Established phase diagram of the $EuBr_2$−CsBr binary system is characterized by the existence of two compounds. First of them, $CsEuBr_3$ undergoes a solid−solid phase transition at 489 K and melts congruently at 1034 K. The second one, $CsEu_3Br_7$, decomposes by peritectoid reaction in the solid state at 864 K.
2. The precise composition of CsBr−$CsEuBr_3$ and $CsEuBr_3$−$EuBr_2$ eutectics corresponding to $EuBr_2$ mole fractions x = 0.197 (T = 812 K) and x = 0.821 (T = 864 K), respectively, was determined from the Tammann diagrams.
3. All the experimental and existing literature data were used for the description of the system under investigation by the CALPHAD method.
4. The agreement of the experimental diagram with the calculated by the CALPHAD method proves the mutual agreement of the obtained thermodynamic data.
5. The calculated mixing entropy of liquid indicates the existence of the $(CsBr)_2(EuBr_2)$ liquid associate.

AUTHOR INFORMATION

Corresponding Author

Leszek Rycerz − *Faculty of Chemistry, Wrocław University of Science and Technology, 50-370 Wrocław, Poland;* orcid.org/0000-0002-2796-848X; Email: leszek.rycerz@pwr.wroc.pl

Authors

Jan Kapała − *Faculty of Chemistry, Wrocław University of Science and Technology, 50-370 Wrocław, Poland*

Marcelle Gaune-Escard − *Ecole Polytechnique, IUSTI CNRS UMR 6595, 13453 Marseille Cedex 13, France*

Complete contact information is available at: https://pubs.acs.org/10.1021/acs.jced.0c01016

Funding

The work was financed by a statutory activity subsidy from the Polish Ministry of Science and Higher Education for the Faculty of Chemistry of Wroclaw University of Science and Technology.

Notes

The authors declare no competing financial interest.

REFERENCES

(1) Dorenbos, P. Energy of the first $4f^7 \rightarrow 4f^6 5d$ transition of Eu^{2+} in inorganic compounds. *J. Lumin.* **2003**, *104*, 239−260.

(2) Terraschke, H.; Wickleder, C. Newest Developments on Eu^{2+}-Doped Nanophosphors. *Chem. Rev.* **2015**, *115*, 11352−11378.

(3) Nano, H. Photostimulable Storage Phosphor Materials and Their Application to Radiation Monitoring. *Sensors Mater.* **2018**, *30*, 327−337.

(4) Maezawa, A.; Mishina, N. Radiation Image Converting Panel and Production Method of the Same. US 6,992,305 B2 2006

(5) Tahon, J. P.; Leblans, P.; Lamotte, J. Method of Preparing Storage Phosphors from Dedicated Precursors. US 0186329 A1 2004

(6) Haschke, J. M.; Eick, H. A. The preparation and some properties of europium bromides and hydrated bromides. *J. Inorg. Nucl. Chem.* **1970**, *32*, 2153−2158.

(7) Rycerz, L.; Kapała, J.; Salamon, B.; Szczygieł, I.; Gaune-Escard, M. Phase diagram and thermodynamic properties of the LaI_3−RbI binary system. *CALPHAD* **2020**, *70*, 101809.

(8) Rycerz, L. *Thermochemistry of lanthanide halides and compounds formed in lanthanide halide-alkali metal halide systems (in Polish). Scientific Papers of Institute of Inorganic Chemistry and Metallurgy of Rare Elements*; Wroclaw University of Technology: Wroclaw 2004.

(9) Rycerz, L. *Thermochemistry of lanthanide halides and their systems with alkali metal halides*; LAP LAMBERT Academic Publishing: Beau Bassin 2017.

(10) JCGM *Evaluation of Measurement Data − Guide to the Expression of Uncertainty in Measurement*; JCGM 2008 *100*.

(11) Pilarek, B.; Rycerz, L.; Chojnacka, I.; Gaune-Escard, M. Enthalpies of mixing in the LaI_3-MI (M = Li, Na, K, Rb, Cs) binary systems. *J. Chem. Eng. Data* **2015**, *60*, 2629−2635.

(12) Findlay, A. *The phase rule and its applications*; Longmans, Green and Co.: New York, 1911.

(13) Rycerz, L. Practical remarks concerning phase diagrams determination on the basis of Differential Scanning Calorimetry measurements. *J. Therm. Anal. Calorim.* **2013**, *113*, 231−238.

(14) Dańczak, A.; Rycerz, L. Reinvestigation of the $DyCl_3$−LiCl binary system phase diagram. *J. Therm. Anal. Calorim.* **2016**, *126*, 299−305.

(15) Seitz, F. *The Modern Theory of Solids*; McGraw-Hill: New York, USA, 1940

(16) Da Silva, F.; Rycerz, L.; Gaune-Escard, M. Calorimetric investgation of MCI-$EuCI_2$ melts (M = Na, K, Rb). *Z. Naturforsch.* **2001**, *56a*, 653−657.

(17) Adya, A.K.; Takagi, R.; Gaune-Escard, M.; Rycerz, L.; Fischer, H. ILL Experimental Report, *Experiment No 6−03-193*, 14−22 May 1996, Grenoble, France

(18) Papatheodorou, G. N.; Kleppa, O. J. Enthalpies of mixing of liquid nickel(II) chloride-alkali chloride mixtures at 810°C. *J. Inorg. Nucl. Chem.* **1970**, *32*, 889−900.

(19) Papatheodorou, G. N.; Kleppa, O. J. Enthalpies of mixing in the liquid mixtures of the alkali chlorides with $MnCl_2$, $FeCl_2$ and $CoCl_2$. *J. Inorg. Nucl. Chem.* **1971**, *33*, 1249−1278.

(20) Kleppa, O. J.; Papatheodorou, G. N. Enthalpies of Mixing of Binary Liquid Mixtures of Cadmium Chloride with Cesium and Lithium Chlorides. *Inorg. Chem.* **1971**, *10*, 872−873.

(21) Kroupa, A. Modelling of phase diagrams and thermodynamic properties using *Calphad* method − Development of thermodynamic databases. *Comput. Mater. Sci.* **2013**, 3−13.

(22) Lukas, H. L.; Fries, S. G.; Sundman, B. *Computational Thermodynamics, The Calphad Method*; Cambridge University Press: Cambridge, 2007.

(23) Lukas, H. L.; Fries, S. G. Demonstration of the Use of "BINGSS" With the Mg-Zn System as Example. *J. Phase Equilib.* **1992**, *13*, 532−542.

(24) Kapala, J. Management Program for BINGSS Phase Diagram Optimizer. *An International Conference on Phase Diagram Calculation and Computational Thermochemistry CALPHAD XXXIII*; Kraków, 30.05−04.06.2004.

(25) Rycerz, L.; Gadzuric, S.; Ingier-Stocka, E.; Berg, R. W.; Gaune-Escard, M. Thermodynamic and structural properties of high temperature solid and liquid $EuBr_2$. *J. Nucl. Mater.* **2005**, *344*, 115−119.

(26) Kubaschewski, O.; Alcock, C. B.; Spencer, P. J. *Materials Thermochemistry*; 6th ed., Pergamon Press: Oxford, 1993.

(27) Sommer, F. Associacion model for the description of thermodynamic functions of liquid alloys part1. *Z. Metallkd.* **1982**, *73*, 72−76.

(28) Sommer, F. Associacion model for the description of thermodynamic functions of liquid alloys. pt 2:Numerical Treatment And Results. *Z. Metallkd.* **1982**, *73*, 77−86.

(29) Krull, H. G.; Singh, R. N.; Sommer, F. Generalised association model. *Z. Metallkd.* **2000**, *91*, 356−365.

(30) Salamon, B.; Rycerz, L.; Kapała, J.; Gaune-Escard, M. Phase diagram of NdI_3−RbI pseudo-binary system. Thermodynamic properties of solid compounds. *Fluid Phase Equilib.* **2015**, *404*, 9−16.

(31) Chojnacka, I.; Rycerz, L.; Kapala, J.; Gaune-Escard, M. Calorimetric investigation of $TmCl_3$-MCl liquid mixtures (M = Li, Na, K, Rb). *J. Mol. Liq.* **2020**, 113935.

https://doi.org/10.1021/acs.jced.0c01016
J. Chem. Eng. Data 2021, 66, 1939−1946